Received: 15 December 2017 | Revised: 16 March 2018 | Accepted: 9 April 2018
DOI: 10.1002/bit.26714

ARTICLE

WILEY BIOTECHNOLOGY BIOENGINEERING

Three-dimensional collagenous niche and azacytidine selectively promote time-dependent cardiomyogenesis from human bone marrow-derived MSC spheroids

Jyotsna Joshi | Gautam Mahajan | Chandrasekhar R. Kothapalli

Department of Chemical and Biomedical Engineering, Cleveland State University, Cleveland, Ohio

Correspondence
Chandrasekhar R. Kothapalli, Department of Chemical and Biomedical Engineering, Cleveland State University, 2121 Euclid Ave. FH 460, Cleveland, OH 44115.
Email: c.kothapalli@csuohio.edu

Funding information
NSF-CBET, Grant number: 1337859
Cellular and Molecular Medicine Specialization fellowship at CSU; NSF-DMR, Grant number: 1126126

Abstract

Endogenous adult cardiac regenerative machinery is not capable of replacing the lost cells following myocardial infarction, often leading to permanent alterations in structure-function-mechanical properties. Regenerative therapies based on delivering autologous stem cells within an appropriate 3D milieu could meet such demand, by enabling homing and directed differentiation of the transplanted cells into lost specialized cell populations. Since type I collagen is the predominant cardiac tissue matrix protein, we here optimized the 3D niche which could promote time-dependent evolution of cardiomyogenesis from human bone marrow-derived mesenchymal stem cells (BM-MSC). 3D collagen gel physical and mechanical characteristics were assessed using SEM and AFM, respectively, while the standalone and combined effects of collagen concentration, culture duration, and 5-azacytidine (aza) dose on the phenotype and genotype of MSC spheroids were quantified using immunofluorescence labeling and RT-PCR analysis. Increasing collagen concentration led to a significant increase in Young's modulus ($p < 0.01$) but simultaneous decrease in the mean pore size, resulting in stiffer gels. Spheroid formation significantly modulated MSC differentiation and genotype, mostly due to better cell–cell interactions. Among the aza dosages tested, 10 μM appears to be optimal, while 3 mg/ml gels resulted in significantly lower cell viability compared to 1 or 2 mg/ml gels. Stiffer gels (2 and 3 mg/ml) and exposure to 10 μM aza upregulated early and late cardiac marker expressions in a time-dependent fashion. On the other hand, cell–cell signaling within the MSC spheroids seem to have a strong role in influencing mature cardiac markers expression, since neither aza nor gel stiffness seem to significantly improve their expression. Western blot analysis suggested that canonical Wnt/β-catenin signaling pathway might be primarily mediating the observed benefits of aza on cardiac differentiation of MSC spheroids. In conclusion, 2 mg/ml collagen and 10 μM aza appears to offer optimal 3D microenvironment in terms of cell viability and time-dependent evolution of cardiomyogenesis from human BM-MSCs, with significant applications in cardiac tissue engineering and stem cell transplantation for regenerating lost cardiac tissue.

KEYWORDS
5-azacytidine, atomic force microscopy, collagen gels, human bone marrow-derived MSCs, myocardial infarction, Wnt signaling

1 | INTRODUCTION

An imbalance between the demand and supply of oxygen in cardiac tissues leads to cardiac ischemia and myocardial cell necrosis, clinically termed as myocardial infarction (MI). MI typically leads to an altered cellular and matrix composition and organization in the myocardium, loss of cardiac tissue, and death of millions of cardiomyocytes (Zimmermann et al., 2006). Among endogenous stem cells native to heart, cardiac stem cells can differentiate into all lineages of heart cells (Bergmann et al., 2009; Hosoda, 2012). However, due to their sparse numbers, the endogenous heart regenerative machinery is not capable of restoring innate structure-function relationship in an injured myocardium. Cardiomyocyte regeneration rate declines with age (1% annually at 25 years to 0.45% annually at 75 years), and that rate is further affected by cardiac-related pathologies (Bergmann et al., 2009; Hosoda, 2012). Additionally, changes in matrix composition, stiffness, and inflammatory environment could adversely impact progenitor cell differentiability in the diseased tissue (Bayomy, Bauer, Qiu, & Liao, 2012). Hence, in conjunction with surgical, pharmaceutical and prosthetic interventions, cellular and tissue engineering based approaches are being explored to control pace of fibrotic cardiac tissue remodeling, prevent the progression of ventricular remodeling, replace the lost cells, and restore the structure-function-mechanical properties of the affected tissue (Chen, Harding, Ali, Lyon, & Boccaccini, 2008; Karam, Muscari, & Montero-Menei, 2012; Karantalis, Balkan, Schulman, Hatzistergos, & Hare, 2012; Russo, Young, Hamilton, Amsden, & Flynn, 2014; Thiene & Basso, 2010).

Various types of stem cells and mature adult cells have been explored for their myocardial regeneration potential (Karam et al., 2012; Karantalis et al., 2012). Among them, human BM-MSCs has been gaining attention in cardiac therapy owing to their relative ease of isolation and expansion, autologous and allogeneic usage, ex vivo modification, and differentiation into cardiomyocyte-like cells under appropriate conditions (Gnecchi, Danieli, & Cervio, 2012; Wang & Guan, 2010). Numerous clinical trials have investigated the utility of human BM-MSCs for cardiac repair; a recent meta-study combining fifty clinical cases on MI and ischemic heart disease reported marginal reduction in infarct size and improvement in the left ventricular ejection fraction with the use of human BM-MSCs (Doppler, Deutsch, Lange, & Krane, 2013). However, reports of inconsistent and transient results from clinical studies of BM-MSC therapy suggest further investigation into the host-cell interactions, mode of cell delivery, and the role of ECM microenvironment (Jadczyk, Faulkner, & Madeddu, 2013; McMullen & Pasumarthi, 2007).

Conventional clinical trials on cellular cardiomyoplasty utilize an isotonic saline solution as a cell delivery vehicle. Such strategies fail to retain large amount of administered cells within the target tissue and maintain their long-term cell viability, since post-infarcted tissue exhibits localized hypoxia, nutrient depletion, inflammatory and oxidative stress, apoptotic cytokines, and fibrotic tissue deposition (Russo et al., 2014). Alternate platforms such as patches or injectables are being explored for cellular delivery, localization, and engraftment to the target site, which could also provide an appropriate 3D niche by supplying biological, pharmaceutical, and mechanical signals to the pathological tissue and aid in tissue regeneration and reversal of adverse ventricular remodeling processes (Arnal-Pastor, Chachques, Pradas, & Vallés-Lluch, 2013; Joshi & Kothapalli, 2015; Lakshmanan, Krishnan, & Sethuraman, 2012).

The utility of collagen-based scaffolds for cardiac tissue engineering merits attention as collagen constitutes around 30% of the total protein in the native cardiac tissue. Type I collagen forms 80% of the total collagen in heart tissue (Li & Guan, 2011; Pelouch, Dixon, Golfman, Beamish, & Dhalla, 1993; Valiente-Alandi, Schafer, & Blaxall, 2016), and plays a critical role in adhesion, proliferation, migration, and various other cellular functions in the embryonic and postnatal myocardium (Pelouch et al., 1993; Valiente-Alandi et al., 2016). In addition to the ECM role in mediating cell–matrix signaling, cell–cell interactions also play a crucial role in stem cell differentiation, especially in controlling mature cardiomyocytes phenotype (Arshi et al., 2013; Gishto, Farrell, & Kothapalli, 2015). A detailed investigation of the role of 3D collagen matrix, cell–cell interactions, and signaling cues on cardiomyogenic differentiation of undifferentiated BM-MSCs is thus warranted from a clinical translational standpoint (Arshi et al., 2013; Potapova et al., 2008).

In this study, we investigated the standalone and combined interactions between cell–matrix (type I collagen gel concentration and stiffness), cell-signaling cues (5-azacytidine dosage), and cell–cell (3D cellular spheroids) interactions, on the time-dependent evolution of cardiomyocytes from human BM-MSC spheroids. 5-azacytidine (aza), an analog of the nucleoside deoxycitidine, is a DNA methyltransferase inhibitor and reportedly changes gene expression via epigenetic process (Goffin & Eisenhauer, 2002). The cardiomyogenic ability of human BM-MSCs were evaluated using varied concentrations and treatment conditions of aza (Martin-Rendon et al., 2008). We hypothesize that a 3D niche provides enhanced differentiation and maturation of MSCs into cardiomyogenic lineage, as cells will experience better autocrine and paracrine signaling with appropriate biomechanical cues. The role of GSK-3β-mediated canonical Wnt-β-catenin pathway and Notch1-DLL4 pathway involved in mediating this process was also elucidated.

2 | MATERIALS AND METHODS

Additional details on the methods listed below was provided in Supplementary Information (online).

2.1 | Preparation and characterization of collagen hydrogels

All reagents and chemicals were purchased from Fisher Scientific (Hanover Park, IL), unless specified otherwise. Corning™ rat tailderived, high-concentration, type-I collagen (Thermo Fisher Scientific, Grand Island, NY) was used to form hydrogels (pH ~7.2) of different concentrations (1, 2, or 3 mg/ml) using procedure recommended by vendor, by adjusting the volumes of collagen, 1 N NaOH, 10× PBS, and sterile distilled water. Collagen gels were imaged using Inspect F50 field-emission SEM (FEI Company, Hillsboro, OR) and

analyzed using ImageJ (NIH). At least five independent SEM images were processed under similar conditions for each hydrogel type to quantify gel features. Young's moduli of the gels were obtained from indentation tests performed on a MFP-3D-Bio atomic force microscope (AFM; Asylum Research, Santa Barbara, CA). Multiple force curves were obtained at random locations for each gel and resulting force versus indentation curves were analyzed by Hertz model fit, using Igor Pro 6.37 software.

2.2 | Human BM-MSC culture, spheroid formation, and differentiation

Cryopreserved Poietics™ normal human BM-MSCs (PT-2501) were obtained from Lonza (Walkersville, MD). Spheroids of human BM-MSCs were formed using a hanging-drop procedure (Sart, Tsai, Li, & Ma, 2014). BM-MSC spheroids were cultured in collagen gels (1, 2, or 3 mg/ml) using a sandwich model and in the presence of 5-aza (0–50 μM, Sigma-Aldrich, St. Louis, MO) over 28 days. The effect of aza and matrix stiffness were quantified using immunofluorescence and RT-PCR (for 10 μM aza treated cases).

2.3 | Immunofluorescence labeling and imaging

Primary antibodies for CD90, GATA4, cardiac Troponin T (cTnT), cardiac Troponin I (cTnI), connexin-43, cardiac myosin heavy chain (MHC), and alpha sarcomeric actin were selected to assess stemness, early, mature and contractile cardiac markers, as per protocols detailed earlier (Gishto et al., 2015). Secondary antibodies used were goat anti-mouse-Texas Red and goat anti-mouse-FITC. The standalone expression and co-expression of the markers was examined using double-immunolabeling and imaging. The standalone expression of the markers would indicate their MSC stemness (CD90), early (GATA 4), or late (cTnT, cTnI) cardiac phenotypes while the co-expression would indicate the heterogeneity of differentiated cells. LIVE/DEAD® Viability/Cytotoxicity Kit (Molecular Probes, Eugene, OR) was used to determine the cellular viability and toxicity at various culture conditions, using protocols optimized earlier (Gishto et al., 2015).

2.4 | RT-PCR analysis for gene expression

Total RNA was extracted from aza-exposed (10 μM) human BM-MSC cultures at 1, 12, and 28-day time points using RNAqueous®-Micro Total RNA Isolation Kit (Thermo Fisher Scientific), as per the vendor specifications. The following genes (Thermo Fisher Scientific) were analyzed: CD90 (Assay ID: Hs00264235_s1), GATA4 (Assay ID: Hs00171403_m1), cardiac troponin T (Assay ID: Hs00943911_m1), and cardiac troponin I (Assay ID: Hs00165957_m1). The expression levels of the target genes were determined using the ΔΔCt method by first normalizing to the endogenous reference gene (18S, Assay ID: 4319413E) and further to aza-free controls.

2.5 | Wnt and Notch signaling pathways

The role of GSK-3β-mediated canonical Wnt/β-catenin pathway was investigated from immuno-fluorescence labeling and Western blots, by quantifying the expression of anti-β-catenin and anti-GSK-3β in respective wells, using the primary antibodies for β-catenin (BD Bioscience, San Jose, CA) and GSK-3β (BD Bioscience). Similarly, the role of DLL4/Notch1 pathway was analyzed using anti-DLL4 and anti-activated Notch1 expressions, with primary antibodies specific for DLL4 (Santa Cruz Biotech, Dallas, TX) and Notch1 (Abcam, Cambridge, MA). Human BM-MSC spheroids were cultured for 6 days in the presence or absence of aza (10 μM), supplemented with or without LiCl (10 mM) or γ-secretase inhibitor (1 μM), to investigate the possible role of Wnt or Notch signaling pathways, respectively.

2.6 | Western blot for protein expression

Spheroids of human BM-MSCs were seeded in 2 mg/ml collagen gels (~40 spheroids per well) in DMEM media, supplemented with or without 5-aza (10 μM), LiCl (10 mM), and γ-secretase inhibitor (1 μM). Samples for Wnt pathway study include: control group, aza-treated group, LiCl treated group, and aza + LiCl treated group (aza exposure for 24 hr followed by its removal and addition of LiCl). Similarly, samples for Notch1 pathway study include: control group, aza-treated group, γ-secretase inhibitor treated group, and aza + γ-secretase inhibitor treated group (aza exposure for 24 hr followed by its removal and addition of γ-secretase inhibitor). SDS/PAGE Western blot analysis was done for semi-quantitative detection of GSK-3β, β-catenin, DLL4, and notch-1 protein bands with their respective primary antibodies (Simmers, Gishto, Vyavahare, & Kothapalli, 2015).

2.7 | Statistical analysis

Data were represented as mean ± standard error, and statistical analysis was performed using GraphPad Prism 5 or SigmaPlot11. Data analysis was performed using Student's *t*-test, or one-way and two-way ANOVA, depending upon the number of groups within a variable, or number of variables to be compared. Appropriate post-hoc tests such as Dunn's multiple comparison, Tukey's multiple comparison, or Bonferroni post-hoc tests were additionally tested to identify any significant differences between the groups. Similarly, three-way ANOVA was implemented followed by Holm–Sidak pair-wise comparisons to find significance between different groups, where appropriate. Differences between data points were considered statistically significant if $p < 0.05$.

3 | RESULTS

3.1 | MSC spheroid cultures within 3D collagen gels

Physical characteristics of the collagen gels at varying concentrations were quantified from the SEM images (Figure 1a) and analyzed using one-way ANOVA followed by Dunn's multiple comparison post-hoc test. Mean pore areas were 0.317, 0.099, and 0.116 μm^2 for 1, 2, and 3 mg/ml hydrogels, respectively, with significant differences ($p < 0.01$) for 1 versus 2 mg/ml, and 1 versus 3 mg/ml gels ($391 \le n \le 636$). On the other hand, mean fiber diameter was 0.09 ± 0.04, 0.14 ± 0.04, and

0.11 ± 0.03 μm for 1, 2, and 3 mg/ml gels, respectively, with differences significant ($p < 0.001$) for 1 versus 2 mg/ml and 2 versus 3 mg/ml gels ($79 \le n \le 95$). Similarly, the average Young's moduli were 113 ± 24.7, 547.1 ± 79.1, and 732.4 ± 50.6 Pa for 1, 2, and 3 mg/ml gels, respectively, with significant differences between each group ($p < 0.05$).

Representative phase-contrast and Live/Dead® assay images of MSC spheroids within 1–3 mg/ml collagen gels were shown in Figure 1b. MSC spheroids cultured on TCP and stained for CD90 demonstrated the stemness of these cells (Figure 1c). Taken together, results suggest that spheroids could be formed from loose MSCs and cultured on TCP or in 3D collagen gels, with no comprise in cell survival. With increasing collagen concentration in the gels, the Young's moduli increased while the mean pore size decreased, indirectly influencing gel stiffness, cell migration and mechanotransduction.

3.2 | Phenotypic and genotypic expression of loose cells versus spheroids

The basal phenotype levels of MSC stemness (CD90), early (GATA4), and late (cTnT/cTnI) cardiomyocyte markers in loose cells (Figure 2a) and spheroids (Figure 2b), cultured on tissue culture plates (TCP) over 24 h, were evaluated using double-immunolabeling and quantified (Figure 2c). CD90 staining was evident with negligible early and late marker expressions in loose cells. MSCs expressing only CD90 were higher in loose cell cultures ($p < 0.01$), while those expressing only GATA4 were higher in spheroids ($p < 0.01$); cells expressing only cTnT or cTnI were negligible in both loose cells and spheroids. Co-expression of the markers were significantly higher in spheroids than in loose cells (Figure 2c; $p < 0.01$) signifying the role of cell–cell interactions in the plasticity and heterogeneity of the spheroids. Gene expressions in 24 hr cultures (Figure 2d) showed detectable amounts of all the four genes tested in both loose cells and spheroids (within first 40 cycles), although cTnI and cTnT expression were significantly higher in spheroids compared to loose cells ($p < 0.01$). GATA4 plays a crucial role in early heart development and is typically expressed in early cardiac progenitors and in the heart from embryonic to postnatal phases (Peterkin, Gibson, Loose, & Patient, 2005). Similarly, cardiac troponins form important components of thin myofibril filaments and contribute to heart muscle contraction (Sehnert et al., 2002). Taken together, these phenotypic and genetic changes attest to the advantages of spheroid 3D culture versus loose cells in 2D cultures, for cardiomyogenic differentiation of human BM-MSCs.

3.3 | Optimization of 5-aza dose within 2 mg/ml collagen gels

The collagen gel concentration was fixed at 2 mg/ml for MSC spheroid cultures, and aza dosage and exposure duration were varied. Based on prior outcomes (Figure 2), MSC spheroids were seeded within 2 mg/ml gels in a 3D sandwich fashion and exposed to varying doses of 5-aza (1, 10, or 50 μM) for up to 28 days, with cultures terminated either after 1-, 12-, or 28-day. Aza-free cultures served as controls and the endpoints such as cell viability, differentiation patterns, phenotypic and genotypic changes under respective conditions were assessed qualitatively and quantitatively at each time point.

Immunofluorescence images of MSC spheroids differentiating under various aza conditions within 1-day cultures were shown in Figure 3a. Within 1-day cultures, ~60% of the cells expressed CD90 in aza-free controls, with ~37% also co-expressing GATA (Figures 3a and 3b). The standalone expression of cTnT was negligible and that of cTnI was low in controls, at the end of 1-day. The co-expression levels of stemness, early, and late markers in control cultures on 1-day were ≥30%. Except within 10 μM aza cultures ($p < 0.05$ for controls vs. 10 μm aza), the presence of aza did not improve the expression of CD90, GATA4, cTnT, or cTnI in 1-day cultures. Also, aza exposure significantly ($p < 0.05$) improved co-expression of markers compared to controls, except for GATA4 + cTnT (Figure 3b). The heterogeneity of cells within spheroids might be playing a major role in day 1 cultures, with or without aza-addition.

Results from 12-day staining (Figures 3c and 3d) showed a significant increase in GATA4 standalone expression ($p < 0.01$ vs. all other aza dosages) and lower CD90 standalone expression, within 10 μM aza-treated group. Although cTnI standalone expression was higher in aza-treated groups ($p < 0.05$ vs. controls), no significant differences in the standalone expressions of CD90 and cTnT nor in their co-expressions were noted with aza exposure. In general, the cytosolic expression of GATA and cTnI increased with aza-treatment and was qualitatively best expressed in 10 μM aza cultures (Figure 3c). Within 28-day cultures, quantification of immunofluorescence images (Figure 3e) indicated low CD90 and cTnT standalone expressions and high GATA4 and cTnI standalone expressions, within cultures receiving aza (Figure 3f). No significant differences were noted in the standalone expressions of CD90, GATA, cTnT, and cTnI nor in their co-expressions, except cTnI in 10 μM aza-treated cultures ($p < 0.01$ vs. controls) where it showed the highest expression.

Gene analysis ($2^{-\Delta\Delta Ct}$ method; Figure 3g) of 10 μM aza-treated cultures in 2 mg/ml collagen gels suggested that compared to aza-free controls: (i) GATA4, cTnI, and cTnT expressions were not detected in 1-day cultures; (ii) a modest but significant increase (2- to 10-fold) in CD90 expression was evident at all time points; (iii) GATA4 expression increased by 2.8- and 234-fold, by 12- and 28-days, respectively; (iv) cTnT expression increased 46- and 21-fold, respectively, by 12- and 28-day; and (v) cTnI expression was undetectable at 12-day, but increased 121-fold by 28-day. A strong positive correlation between gene and protein expressions of GATA and cTnI in 28-day cultures was evident. LIVE/DEAD® analysis showed high viability (>75%) in all cultures, with no dependence on aza-concentration or culture duration (Figure 3h). Taken together, MSC spheroids in 2 mg/ml collagen gels supplemented with 10 μM aza evolved with significant standalone GATA4 and cTnI expression with culture duration, but with no compromise in cell viability.

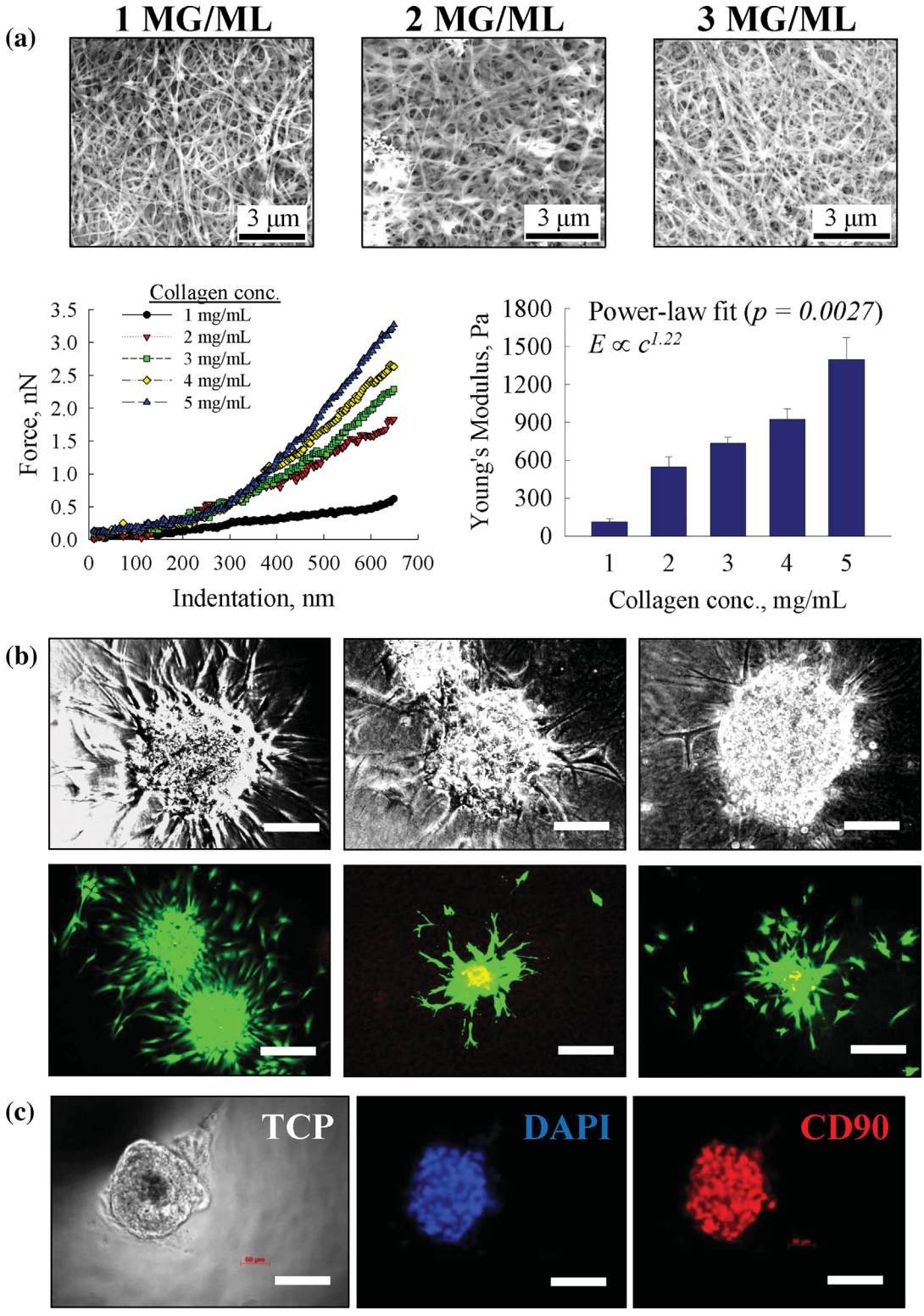

FIGURE 1 (a) Representative SEM images of the collagen gels prepared at varying concentrations (1–3 mg/ml). Representative force-indentation curves from AFM analysis were shown for collagen gels prepared over a wide range of concentrations. A systematic increase in slope of the curves is evident with increasing concentration. The Young's modulus calculated from these curves ranged between 50–1,400 Pa for the gel concentrations tested here. The data were fit to a power-law fit ($p = 0.0027$) which showed that $E \propto c^{1.22}$. (b) Representative phase-contrast images of human BM-MSC spheroids, formed using hanging-drop protocol and seeded for 24 hr in 1–3 mg/ml collagen gels. Representative LIVE/DEAD® stained images of the spheroids were also shown in these gels under respective culture conditions. (c) Representative phase-contrast (left), DAPI (middle), and CD90 (right) stained images of BM-MSC spheroids, cultured for 24 hr on tissue culture polystyrene (TCP). Scale bars: 100 μm. At least three gels were characterized for each experiment, and experiments were done in triplicate

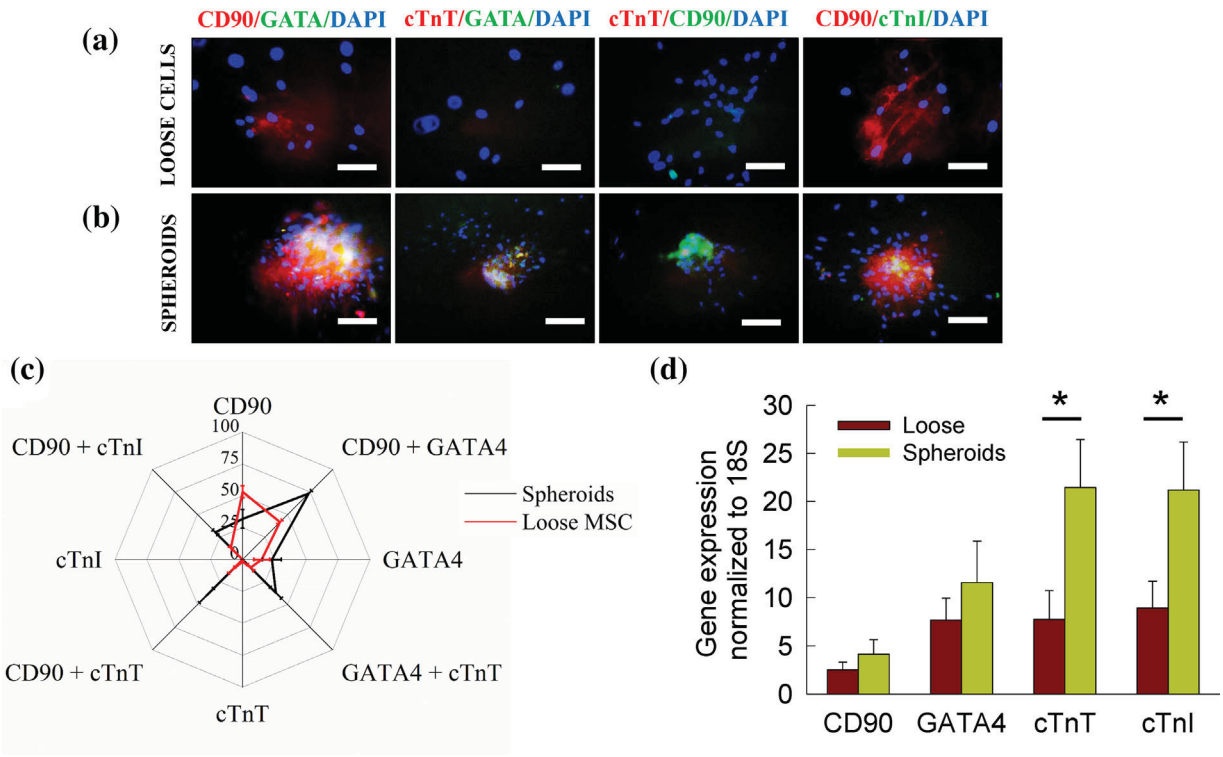

FIGURE 2 Representative immunofluorescence images of MSC stemness (CD90), early (GATA4), and late (cTnT/cTnI) cardiomyocyte markers in loose cell cultures (a) and in spheroids (b), cultured on tissue culture polystyrene plates (TCP) for 24 hr. Scale bar: 100 μm. (c) Radar plot showing quantification of the phenotypic expression of these markers using double-immunolabeling procedures. Data shown represents average ± standard error. (d) Gene-expression analysis of the cardiomyocyte markers in 24 hr cultures performed using ΔCt method. * indicates $p < 0.05$ between cases. At least three independent wells were characterized for each experiment, and experiments were done in triplicate

3.4 | Effect of 1 mg/ml collagen on MSC survival, phenotype, and genotype

After identifying optimal aza dose, the role of collagen gel stiffness on human BM-MSC differentiation, phenotype and genotype was investigated. MSC spheroids were seeded in type I collagen (1 or 3 mg/ml) in a 3D sandwich model and exposed to 10 μM aza for over 28 days, while aza-free cultures served as respective controls. Figure 4 shows the outcomes within 1 mg/ml collagen cultures, at 1, 12, and 28-day time points, in the presence or absence of 10 μM aza.

Within 1-day cultures, significant presence of CD90 was noted within controls, either as standalone or in conjunction with GATA4 expression (Figures 4a and 4b). The standalone and co-expressions of cTnT and cTnI were low in these control cultures. The presence of aza showed similar trends in the standalone and co-expression of markers, except for higher co-expression of CD90 + cTnI ($p < 0.001$ vs. controls; Figure 4b). Immunostaining results from 12-day cultures (Figures 4c and 4d) suggested no significant differences between controls and 10 μM aza-receiving cultures, for the standalone and co-expressions of all four markers. Significant improvement was seen in the standalone expression of CD90 and co-expressions of CD90 + GATA4, GATA4 + cTnT, and CD90+ cTnT (Figures 4e and 4f) with aza addition in 28-day cultures. GATA + cTnT was almost three times higher with aza-treatment compared to controls ($p < 0.001$).

RT-PCR analysis of MSCs exposed to 10 μM aza in 1 mg/ml collagen gels (Figure 4g) showed (i) no significant changes in CD90 gene expression at all time points compared to controls; (ii) an almost 820-fold increase in GATA4 expression by 1-day, which significantly decreased by 12 and 28-days; (iii) significant increases in cTnT expression on 1-day (820-fold) and 12-day (1,020-fold); and (iv) significantly higher cTnI expressions on 1-day (167-fold) and 12-day (1,020-fold). A strong positive correlation between gene and protein expressions of all tested markers was noted in 1- and 12-day cultures. LIVE/DEAD® assay showed viability >80% in all cultures over the duration of 28-days, without any significant difference between controls and aza-exposed cultures (Figure 4h). Taken together, MSC spheroids in 1 mg/ml gels and aza exposure evolved with culture duration as heterogeneous cells with both stemness and cardiac phenotypes, with no compromise in cell viability.

3.5 | Effect of 3 mg/ml collagen on MSC survival, phenotype, and genotype

Within 1-day cultures, the standalone expression of CD90 and GATA4 was evident in both controls and aza-additive cultures, but that of cTnI and cTnT was negligible (Figures 5a and 5b). The co-expression levels of stemness, early, and late markers in controls and aza-receiving cultures were higher, similar to that noted in 1 and 2 mg/ml gels.

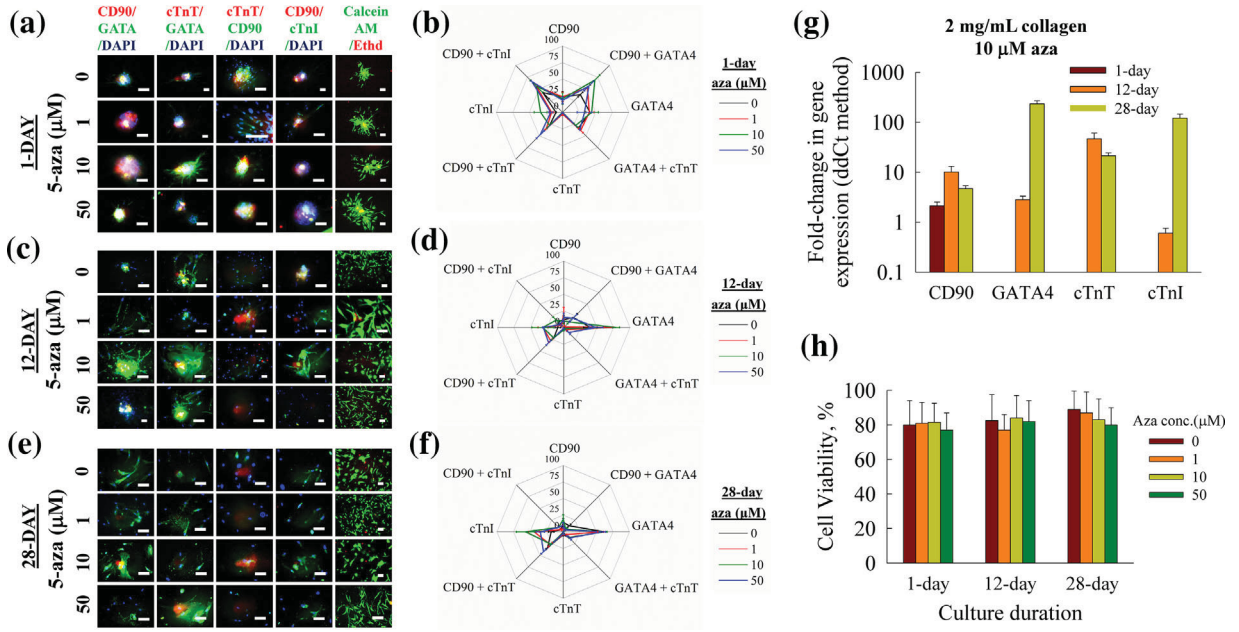

FIGURE 3 Representative immunofluorescence images of MSC spheroids cultured in 2 mg/ml collagen gels, and double-stained for stemness (CD90), early (GATA4), and late (cTnT, cTnI) cardiomyocyte differentiation markers, at 1-day (a), 12-day (c), and 28-day (e) timepoints. Aza-concentration was varied from 0 to 50 μM at all time points. Cells were counterstained with DAPI to detect nuclei. Representative images from the Live/Dead® assay, to assess cell viability under respective culture conditions, were also shown. Scale bar: 100 μm. Radar plots showing quantification of the phenotypic expressions of these markers in 1-day (b), 12-day (d), and 28-day (f) cultures within 2 mg/ml collagen gels. Data shown represents average ± standard error. (g) Gene expression of the four markers in MSC spheroids cultured within 2 mg/ml gels and exposed to 10 μM aza was quantified using $2^{-\Delta\Delta Ct}$ method. Data shown represents average ± standard deviation. (h) Cell viability under different culture conditions within 2 mg/ml collagen gels was quantified. Data shown represents average ± standard deviation. At least three independent gels were characterized for each experiment, and experiments were done in triplicate

However, there was no significant difference in the standalone and co-expression levels of markers between controls and aza-treated cultures on day 1. Within 12-day cultures, no significant differences between controls and aza-treated cells were noted (Figures 5c and 5d). Except CD90, the standalone expression of all the three markers was negligible in all cases studied. However, the co-expression levels were detectable, with CD90 + GATA4 and GATA + cTnT being higher in controls, while CD90 + cTnT and CD90 + cTnI being higher in aza-receiving cultures. By 28-day, CD90 and cTnT standalone expressions were almost negligible in controls and aza-added cultures (Figures 5e and 5f). While GATA4 standalone expression was similar in controls and aza-added cultures, cTnI standalone expression significantly improved with aza exposure ($p < 0.01$ vs. controls). The co-expression levels of markers were low in all the cases (<20%), except for CD90 + cTnI, which was higher upon aza-exposure.

RT-PCR analysis (Figure 5g) suggested that in the presence of aza, CD90 gene expression was slightly upregulated in 1- and 28-day cultures, while increases (nine-fold) in GATA4 and cTnT expressions were noted only in 28-day cultures. However, cTnI gene expression increased significantly by 12-day (24.5-fold) and almost 207-fold by 28-days. A strong positive correlation between gene and protein expressions of CD90 on 1-day, and cTnI and GATA4 on 28-day was noted. Cell survival studies showed viability >70% in all the cases except for aza-receiving 28-day cultures (Figure 5h). Comparing cell viability among all culture conditions (1, 2, or 3 mg/ml gels, with or without aza), 3 mg/ml cultures exposed to 10 μM aza showed significantly lower cell viability. Taken together, MSC spheroids in 3 mg/ml gels evolved with higher standalone and co-expression of cTnI with aza-treatment, but showed significant reduction in cell viability. The statistical analysis of these results presented thus far was provided in online supplementary information.

3.6 | Expression of cardiac conduction and contractile proteins

MSC spheroids were seeded in collagen gels in a 3D sandwich model and exposed to 5-aza (0 or 10 μM) over 28 days. Cultures from 12- and 28-day were compared to analyze the qualitative expression of mature cardiac marker expression (Figure 6a–c; Cx43, MyHC, α-actin). A strong nuclear localization of connexin-43 was noted in 1 and 2 mg/ml gels by 12-day, which also localized along the cytoplasmic regions by 28-day, in both controls and aza-treated cultures (Figures 6a and 6b). Cx43 expression in cardiomyocytes obtained from adipose tissue-derived MSCs via 5 μM aza-treatment was largely confined in nuclear and cytoplasmic membranes and at junctions of adjacent cells (Carvalho et al., 2013). In our study, we did not detect significant differences in Cx43 expression among different culture conditions. Based on prior observations that Cx43 protein was upregulated upon cell–cell contact

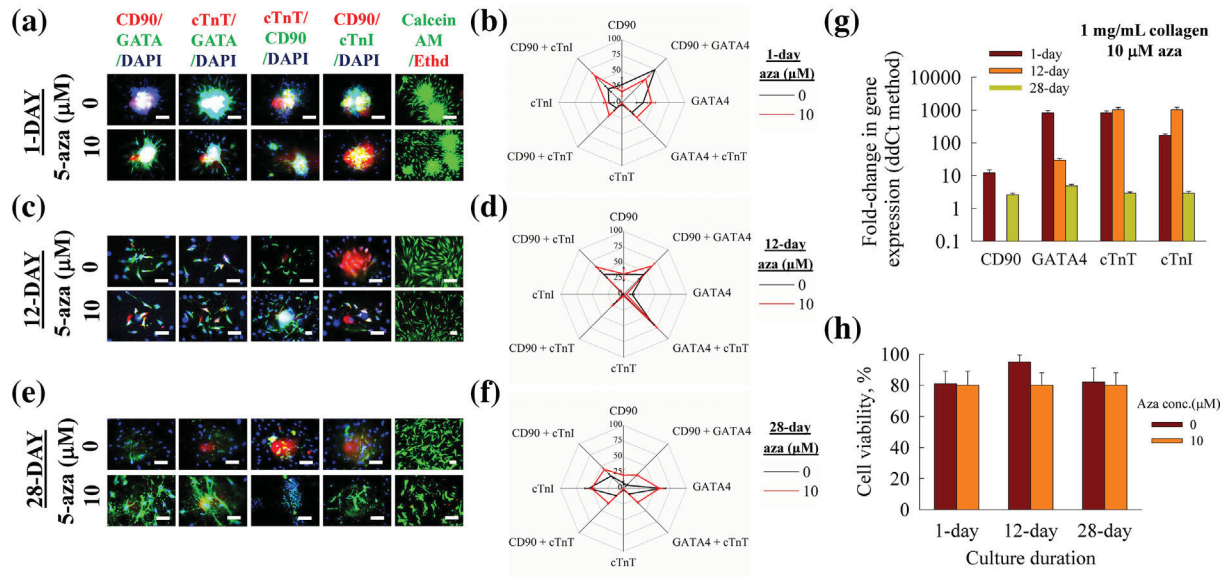

FIGURE 4 Representative immunofluorescence images of MSC spheroids cultured in 1 mg/ml collagen gels, double-stained for stemness (CD90), early (GATA4), and late (cTnT, cTnI) cardiomyocyte differentiation markers, at 1-day (a), 12-day (c), and 28-day (e) timepoints. Aza-concentration was either 0 or 10 μM at all time points. Cells were counterstained with DAPI to detect nuclei. Representative images from the Live/Dead® assay, to assess cell viability under respective culture conditions, were also shown. Scale bar: 100 μm. Radar plots showing the quantification of the phenotypic expressions of these markers in 1-day (b), 12-day (d), and 28-day (f) cultures within 1 mg/ml collagen gels. Data shown represents average ± standard error. (g) Gene expression of the four markers in MSC spheroids cultured within 1 mg/ml gels and exposed to 10 μM aza was quantified using $2^{-\Delta\Delta Ct}$ method. Data shown represents average ± standard deviation. (h) Cell viability under different culture conditions within 1 mg/ml collagen gels was quantified. Data shown represents average ± standard deviation. At least three independent gels were characterized for each experiment, and experiments were done in triplicate

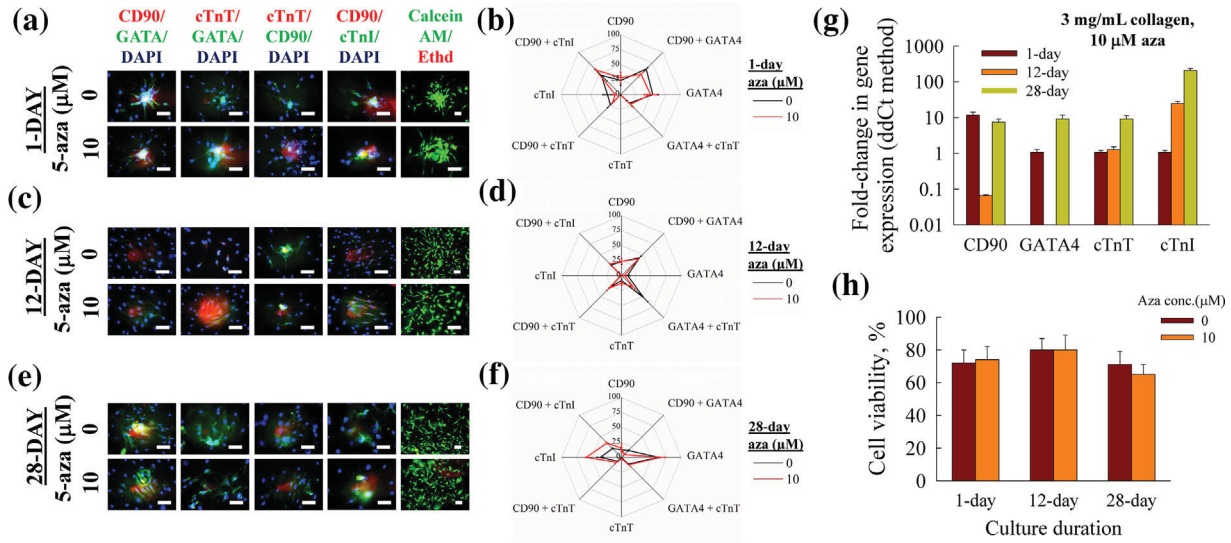

FIGURE 5 Representative immunofluorescence images of MSC spheroids cultured in 3 mg/ml collagen gels, double-stained for stemness (CD90), early (GATA4), and late (cTnT, cTnI) cardiomyocyte differentiation markers, at 1-day (a), 12-day (c), and 28-day (e) timepoints. Aza-concentration was either 0 or 10 μM at all time points. Cells were counterstained with DAPI to detect nuclei. Representative images from the Live/Dead® assay, to assess cell viability under respective culture conditions, were also shown. Scale bar: 100 μm. Radar plots showing the quantification of the phenotypic expressions of these markers in 1-day (b), 12-day (d), and 28-day (f) cultures within 1 mg/ml collagen gels. Data shown represents average ± standard error. (g) Gene expression of the four markers in MSC spheroids cultured within 3 mg/ml gels and exposed to 10 μM aza was quantified using $2^{-\Delta\Delta Ct}$ method. Data shown represents average ± standard deviation. (h) Cell viability under different culture conditions within 3 mg/ml collagen gels was quantified. Data shown represents average ± standard deviation. At least three independent gels were characterized for each experiment, and experiments were done in triplicate

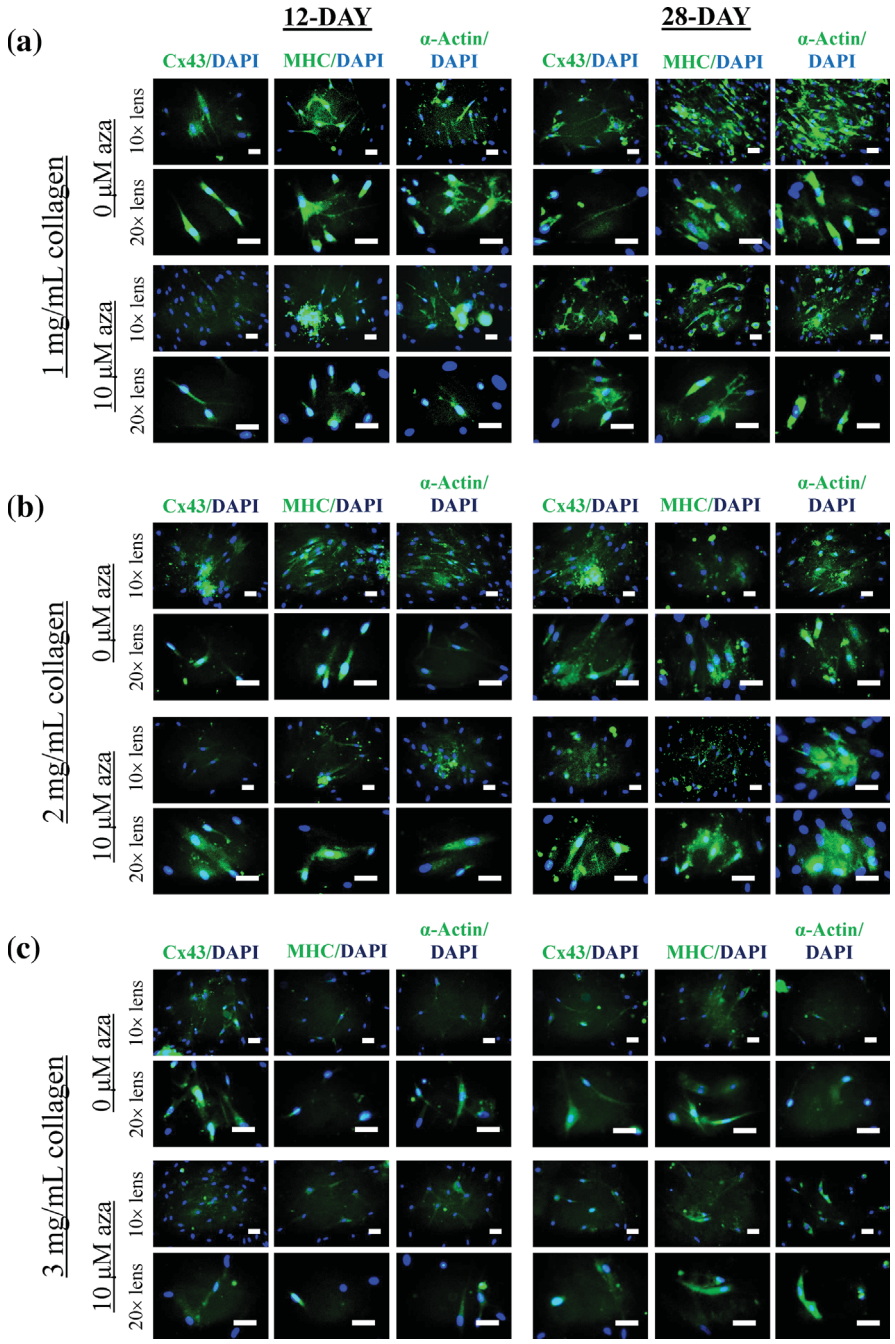

FIGURE 6 Representative immunofluorescence images of BM-MSC spheroids cultured in 1 mg/ml (a), 2 mg/ml (b), or 3 mg/ml (c) collagen gels, in the presence of either 0 or 10 μM aza, for 12- or 28-days, and stained for mature cardiac markers such as connexin-43 (Cx43), cardiac myosin heavy chain (MHC), and sarcomeric α-actin. Two different magnifications (10× and 20×) were shown for each staining marker at each culture condition. Scale bar: 100 μm. At least three independent gels were characterized for each experiment, and experiments were done in duplicate

in 3D MSC aggregates (Sart et al., 2014), it could be inferred that cell–cell interactions in MSC spheroids and type I collagen gels play a strong role in inducing Cx43 expression. A strong nuclear localization of MHC and sarcomeric α-actin proteins was noted within 1 mg/ml collagen cultures by 12-day in the presence or absence of aza, which also localized along the cytoplasm by 28-day (Figure 6a). On the other hand, the cytosolic expression of α-actin appeared to improve with aza addition in 12-day cultures within 2 mg/ml gels, and in 28-day cultures in 3 mg/ml gels. Taken together, MSC spheroids and collagen type I appeared to play major role in the expression of cardiac conduction and contractile marker and seem to be independent of gel stiffness.

3.7 | Role of Wnt/β-catenin signaling pathway

We examined the possible role of GSK-3β-mediated canonical Wnt/β-catenin signaling pathway in collagen gel stiffness and aza-induced

cardiomyogenic differentiation of human BM-MSC spheroids. One-way ANOVA followed by Tukey's post hoc test was ran to find significant differences in the expression of major components of Wnt pathway, in cultures treated with or without aza, and with or without the respective inhibitors or activators of the pathway. Immunofluorescence labeling and quantification showed glycogen synthase kinase (GSK-3β) expression to be the lowest in LiCl-receiving cultures ($p < 0.01$ vs. controls), with the highest expression in aza-treated group ($p < 0.05$ vs. controls) followed by aza + LiCl cultures (Figures 7a and 7b). This was to be expected because aza was shown to increase GSK-3β expression while LiCl supposedly inhibits that expression. The rescue of GSK-3β expression by aza in LiCl cultures ($p < 0.05$ vs. LiCl culture) confirms that 5-aza indeed modulates MSCs via GSK-3β pathway. Western blot analysis (Figure 7d) of GSK-3β protein in cell lysates, under respective conditions, confirmed the trends noted from fluorescence imaging. Similarly, significant differences in β-catenin expression (Figure 7a–c) was noted between aza-treated group versus controls ($p < 0.05$), and aza-treated group versus LiCl-treated group ($p < 0.05$). Western blot analysis (Figure 7e) of β-catenin protein in cell lysates suggested that exposure to aza alone, LiCl alone, or aza + LiCl suppressed β-catenin levels ($p < 0.01$ for all cases vs. controls). Interestingly, addition of LiCl alone significantly inhibited β-catenin protein expression, which was rescued by the addition of aza (Figure 7e).

In a similar vein, aza caused a significant upregulation of GSK-3β but a concomitant down-regulation of β-catenin, while also inducing

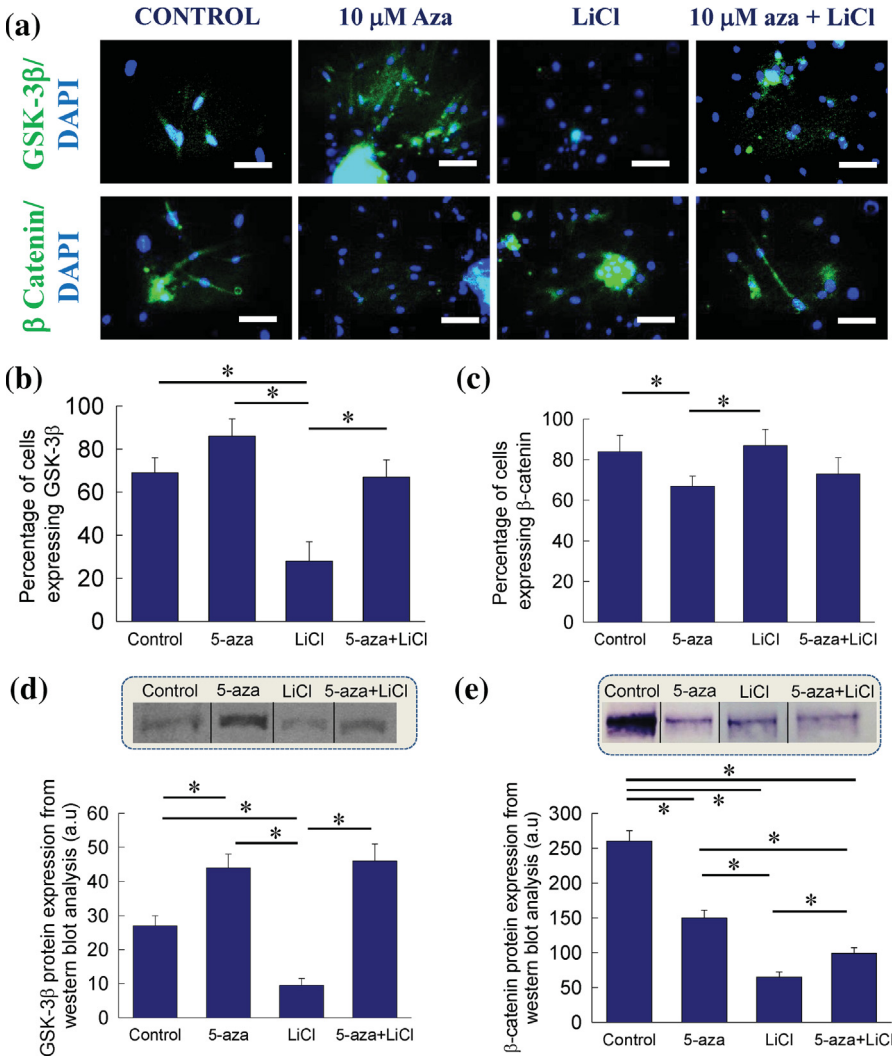

FIGURE 7 (a) Representative immunofluorescence images of the major proteins involved in GSK-3β-mediated canonical Wnt-β-catenin signaling pathway. MSC spheroids were cultured for 6 days in 2 mg/ml collagen gels, and exposed to either 10 μM aza, or LiCl, or both. Control cultures received neither aza nor LiCl. Cells were counterstained with DAPI for nuclei staining. Scale bar: 100 μm. Percentage of cells expressing GSK-3β (b) and β-catenin (c) were quantified under respective culture conditions from these images. Semi-quantitative Western blot analysis was performed to quantify the expression of GSK-3β (d) and β-catenin (e) levels in respective cultures. Representative western blot bands for each condition were shown in the inset for comparison. These bands were taken from the same gels, but from different lanes, as gels were loaded in duplicate for each condition. * indicates $p < 0.05$ between cases. At least three independent gels were characterized for each experiment, and experiments were done in duplicate

cardiac-specific genes in mouse BM-MSCs (Cho, Rameshwar, & Sadoshima, 2009). Furthermore, aza-induced cardiomyogenic gene expression was suppressed upon exposure to LiCl (GSK-3β inhibitor), and also upon the specific knock-down of GSK-3β (Cho et al., 2009). Taken together, aza-treatment facilitated GSK-3β-induced phosphorylation and degradation of β-catenin expression compared to controls, attesting to the specific role of aza-induced Wnt/β-catenin signaling pathway on cardiomyogenesis of human BM-MSC spheroids.

3.8 | Role of DLL4/Notch signaling pathway

Immunofluorescence staining did not show any significant differences in DLL4 expression among the culture groups (Figures 8a and 8b), but a significant difference in the expression of activated Notch1 between γ-secretase-inhibitor (presence and absence of aza) and control cultures (Figure 8a–c). Previous studies attest to the inhibitory role of Notch signaling during heart development as well as during cardiomyogenic differentiation of embryonic stem cells (Perino, Yamanaka, Li, Wobus, & Boheler, 2008). In contrast, significant upregulation in Notch1, DLL4, Nkx 2.5, and GATA4 gene expressions were noted in aza-treated human umbilical cord-derived MSCs compared to controls (Ruan, Zhu, Yin, & Chen, 2010). In line with their findings, we noted slightly higher activated Notch1 expression in aza-treated cultures compared to controls (74% vs. 65%). We also noted significantly higher Notch1 expression in the presence of γ-secretase inhibitor, which is surprising because the epitope of activated Notch 1 is supposed to be exposed only after γ-secretase cleavage and is not accessible in the uncleaved form (Koyanagi et al., 2007). Activation of Notch1 in aza-treated group compared to controls would suggest better cardiac differentiation outcomes with 5-aza treatment, but higher Notch1 expression in γ-secretase inhibitor treated samples also suggests a dominant role of cell–cell or cell–ECM interactions in MSC spheroids which might have counteracted the effect of γ-secretase inhibition and instead accelerated Notch-activation via some hitherto unknown mechanisms.

4 | DISCUSSION

Studies have shown that MSC spheroids exhibit enhanced anti-inflammatory, angiogenic, and differentiation potential (Bartosh et al., 2010; Cesarz & Tamama, 2016). Specifically, human MSC spheroids showed detectable amounts of cardiac proteins such as sarcomeric α-actinin, troponin-T, and atrial natriuretic peptide, whereas their loose counterparts did not (Potapova et al., 2008). MSCs within spheroids would experience greater cell–cell interactions while loose MSCs would experience mostly cell–matrix interactions. In 2D loose cultures on TCP, MSCs directly attach and sense the high elastic modulus (GPa range) of the substrate, whereas cells within spheroids attach to neighboring cells and ECM which have significantly lower elastic modulus (Cesarz & Tamama, 2016). Thus, the type of MSC culture (loose vs. spheroid) would influence the expression levels of receptors/ligands for cell–cell interactions or for cell–matrix adhesion, which will influence their functions such as adhesion, proliferation, migration, and differentiation. In our study, on day 1, compared to loose MSCs, spheroids exhibited better cardiogenic potential as evident from their genotypic and phenotypic expressions. In addition, spheroids expressed cardiac conduction and contractile markers which were not significantly influenced by scaffold stiffness and aza-addition, suggesting the standalone role of spheroids in cardiomyogenesis.

The effect of cardiogenic factors such as 5-aza on MSC differentiation has been reported earlier. Beating cardiomyogenic cells were formed from murine bone marrow stromal cells after 2 weeks of culture, following treatment with 3 μM aza for 24 hr (Makino et al., 1999). However, treatment with aza for 24 h did not result in tropomyosin expression in cord blood and umbilical cord-derived MSCs even after 4-weeks of cultures, while bone marrow-derived MSCs differentiated to tropomyosin-positive cells at concentrations ≥5 μM aza (Martin-Rendon et al., 2008). On the other hand, continuous exposure to aza resulted in greater cell death, while single exposure to aza caused relatively smaller fraction of MSCs to differentiate into immature phenotype (Piryaei et al., 2015). Although we noted the potential advantages of aza dosage and treatment duration on the cardiogenic differentiation of human BM-MSCs, the outcome was also dependent on collagen gel stiffness. In 2 mg/ml gels, 10 μM aza proved optimal as it led to time-dependent evolution of cardiomyogenesis (cells exhibited highest standalone expression of GATA4 by 12-day and cTnI by 28-day). However, such benefits of 10 μM aza was not examined in 1 mg/ml gels, where heterogeneous phenotypes evolved even on 28-day. In contrast, aza supplementation caused higher cTnI expression by 28-day in 3 mg/ml gels, as evident from gene and protein studies, but with significant cell viability reduction. Despite continuous exposure of MSCs to aza for up to 4-weeks, we did not observe any negative impact of 5-aza on MSC viability within softer gels (1 and 2 mg/ml) suggesting higher spheroid integration rate in gels compared to loose cells (Sart et al., 2014).

Substrate stiffness is an important determinant in cardiac differentiation as it plays a crucial role in ligand presentation, cardiomyogenic differentiation, maturation, and homeostasis during developmental, postnatal, and post-infarct stages (Forte et al., 2012; Hazeltine et al., 2012; Qiu et al., 2015). Here, we varied the concentration of collagen gel to examine the role of 3D niche stiffness on cardiac differentiation of MSCs. We noted the Young's moduli of collagen gels to increase monotonously with concentration (1 to 5 mg/ml), with a power-law dependence ($E \propto c^{1.22}$; $p = 0.002$), as evident from AFM indentation tests. Prior studies suggest that the storage moduli of collagen gels increased with concentration ($G' \sim c^{2.1}$, at 37 °C) (Yang, Leone, & Kaufman, 2009); the shear moduli (G') of 1, 2, and 3 mg/ml collagen gels at low strain (0–0.1) were reported as 3, 44.5, and 97 Pa, respectively, while their respective tensile modulus (E) at 0.1 mm/min strain rate were reported in 10–17 KPa range (Lee et al., 2014; Lopez-Garcia, Beebe, & Crone, 2010).

Immunolabeling studies showed that cTnT expression in 12-day cultures within 3 mg/ml gels was the highest, compared to 1 or 2 mg/ml collagen cultures; yet, the standalone expression of cTnT was not sustained till day 28. MSC spheroids evolved to acquire cardiac phenotype by 28-day in all the gels suggesting that matrix stiffness and

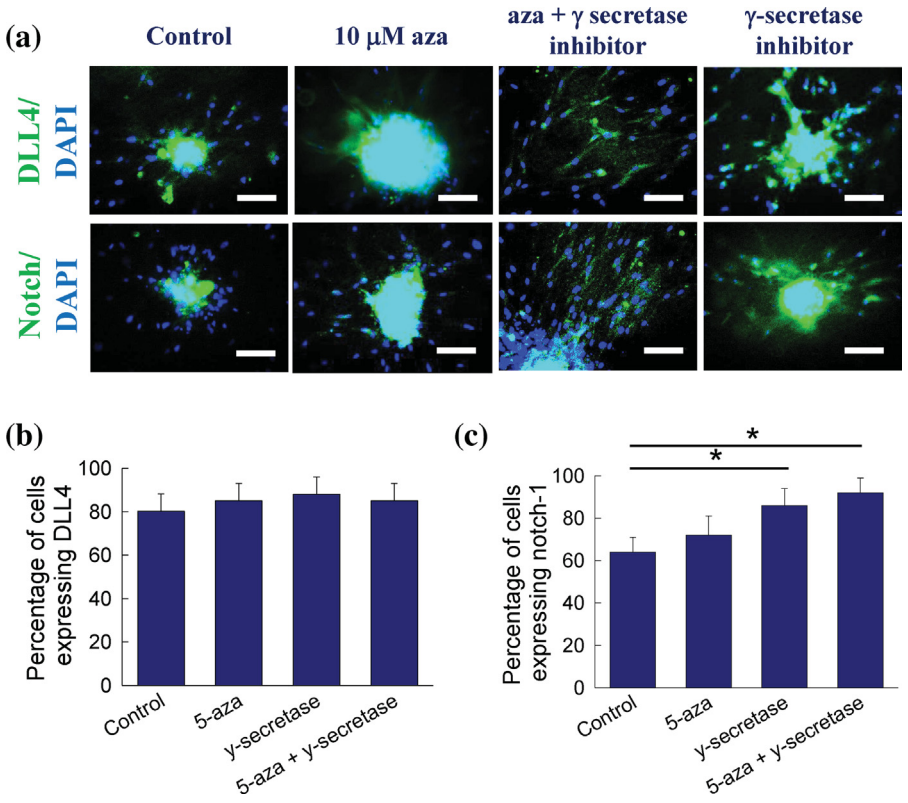

FIGURE 8 (a) Representative immunofluorescence images of the major proteins involved in Notch1-DLL4 signaling pathway. MSC spheroids were cultured for 6 days in 2 mg/ml collagen gels, and exposed to either 10 μM aza, or γ-secretase, or both. Control cultures received neither aza nor γ-secretase. Cells were counterstained with DAPI for nuclei detection. Scale bar: 100 μm. Percentage of cells expressing DLL4 (b) and notch-1 (c) were quantified under respective culture conditions from these images. * indicates $p < 0.05$ between cases. At least three independent gels were characterized for each experiment, and experiments were done in duplicate

matrix type could play a role in cardiomyogenesis. Spheroids within stiffer hydrogels (2 and 3 mg/ml) and aza-exposure exhibited higher standalone expressions of cTnI by 28-day, whereas those within 1 mg/ml gels evolved to heterogeneous cell phenotypes, suggesting the combined role of matrix stiffness and signaling cues on cardiomyogenesis. Significant reduction in cell viability within 3 mg/ml gels by day 28, with or without aza addition, indicates that higher gel concentration could limit adequate diffusion of nutrients to the cells. Such reduction in viability could also be due to lower cell proliferation, or higher MSC differentiation into cardiac like cells, or reduced oxygen levels for cells inside the spheroid within stiffer (and low porosity) gels. Regardless, compromise in cell viability within stiffer matrices indicates one limitation of 3 mg/ml gels for cell replacement therapy applications.

While the cell viability and standalone expression of cardiac markers (GATA4 and cTnI) were influenced by matrix stiffness, aza dosage, and treatment duration, cardiac conduction and contractile markers expression seems to be largely dependent on spheroid formation and collagen culture alone (independent of gel stiffness). This suggests that specific microenvironmental factors such as cell–cell and cell–ECM interactions, matrix rigidity, dosage, and duration of signaling cues, or their combined interactions, have major influence on the expression of cardiac phenotypic and genotypic traits.

In all the culture conditions tested in this study, the standalone expression of cTnT by 28-day remained quite low, indicating that additional stimuli (mechanical, chemical, or biological) might be needed to guide and sustain cTnT expression within human BM-MSC cultures. Other researchers have shown that besides aza, biochemical molecules such as phorbol myristate acetate, bFGF, hydrocortisone, or BMP-2 enhance cTnT expression in cardiomyocytes derived from MSCs (Hafez et al., 2016; Hou et al., 2013; Seo et al., 2016). Our future studies are geared toward elucidating the influence of a combination of mechanical stimuli and paracrine signaling on cTnT expression in these cultures. The Young's moduli of 1–3 mg/ml collagen gels we tested ranged within 100–800 Pa, while that of the native heart evolves from a softer mesodermal layer tissue with low stiffness (≈500 Pa) to a contractile tissue with higher stiffness (≈10 kPa) by E14 (Young, Kretchmer, Ondeck, Zambon, & Engler, 2014). Hence, clinical translation of pure collagen gel based therapies could be limited by their inherently low mechanical properties as these gels have to sustain the continuous beating of the heart once implanted, and also lack the control on biodegradation in vivo. Such discrepancy in Young's moduli between in vitro approaches and native tissue is also because cardiac ECM is not only a mesh of type I collagen, but also consists other matrix proteins such as type III collagen, elastin, laminin, fibrillin, fibronectin, and GAGs. These limitations could partially be overcome by tuning the chemical/physical cross-linking of collagen gels, or by altering the gel geometry, or blending collagen with other biopolymers such as GAGs or elastin (Parenteau-Bareil, Gauvin, & Berthod, 2010). Hence, future investigations on the standalone and the combined role of multiple

cardiac proteins-derived hydrogels will lead to enhanced knowledge for clinical translation.

5 | CONCLUSIONS

We noted significant standalone and combined effects of collagen gel concentration, aza dosage, exposure duration and cell–cell interactions, on the cardiomyogenic evolution of human BM-MSCs. MSC spheroids facilitated better differentiation indicating the strong role of intimate cell–cell contact on the genotypic and phenotypic progression of MSCs toward cardiomyogenic lineage. Within 2 mg/ml collagen gels, 10 μM aza promoted time-dependent evolution of early and late cardiac markers, whereas aza-addition to 1 mg/ml gels promoted heterogeneous cell populations with both stem and cardiac like phenotypes by 28-day, highlighting the combined role of matrix stiffness and signaling cues on cardiac differentiation. Within 3 mg/ml collagen gels, aza addition offered significant benefit to cTnI gene and protein expression by 28-days, but cell viability was significantly compromised. On the contrary, spheroid culture alone seems to play major role in the expression of cardiac conduction and contractile markers, which appear to be independent of gel stiffness. Taken together, results from our study attest to the standalone and the combined role of 3D microenvironmental variables (spheroid culture, collagen stiffness, aza concentration. and treatment duration) in influencing the cardiomyogenic differentiation and maturation of human BM-MSC spheroids, with potential applications in regenerating ischemic cardiac tissues following MI.

ACKNOWLEDGMENTS

C.K. expresses his gratitude to the CSU Office of Research funds and partial funding from NSF-CBET (Grant number 1337859). J.J. would like to thank the financial support from the Cellular and Molecular Medicine Specialization fellowship at CSU. The authors would like to thank Drs. Crystal Weyman and Sailen Barik (Biology, CSU) for providing access to the RT-PCR facilities, and Dr. Petru Fodor for access to the field-emission SEM facility (funded by NSF-DMR grant number 1126126).

ORCID

Chandrasekhar R. Kothapalli http://orcid.org/0000-0001-8450-0640

REFERENCES

Arnal-Pastor, M., Chachques, J. C., Pradas, M. M., & Vallés-Lluch, A. (2013). Biomaterials for cardiac tissue engineering. *Regenerative Medicine and Tissue Engineering*, *1*, 275–303.

Arshi, A., Nakashima, Y., Nakano, H., Eaimkhong, S., Evseenko, D., Reed, J., … Nakano, A. (2013). Rigid microenvironments promote cardiac differentiation of mouse and human embryonic stem cells. *Science and Technology of Advanced Materials*, *14*(2), 025003.

Bartosh, T. J., Ylostalo, J. H., Mohammadipoor, A., Bazhanov, N., Coble, K., Claypool, K., … Prockop, D. J. (2010). Aggregation of human mesenchymal stromal cells (MSCs) into 3D spheroids enhances their antiinflammatory properties. *Proceedings of the National Academy of Sciences of the United States of America*, *107*(31), 13724–13729.

Bayomy, A. F., Bauer, M., Qiu, Y., & Liao, R. (2012). Regeneration in heart disease—Is ECM the key? *Life Sciences*, *91*(17), 823–827.

Bergmann, O., Bhardwaj, R. D., Bernard, S., Zdunek, S., Barnabé-Heider, F., Walsh, S., … Frisén, J. (2009). Evidence for cardiomyocyte renewal in humans. *Science*, *324*(5923), 98–102.

Carvalho, P. H., Daibert, A. P., Monteiro, B. S., Okano, B. S., Carvalho, J. L., Cunha, D. N., … Del Carlo, R. J. (2013). Differentiation of adipose tissue-derived mesenchymal stem cells into cardiomyocytes. *Arquivos Brasileiros de Cardiologia*, *100*(1), 82–89.

Cesarz, Z., & Tamama, K. (2016). Spheroid culture of mesenchymal stem cells. *Stem Cells International*, *2016*, 9176357.

Chen, Q.-Z., Harding, S. E., Ali, N. N., Lyon, A. R., & Boccaccini, A. R. (2008). Biomaterials in cardiac tissue engineering: Ten years of research survey. *Materials Science and Engineering: R: Reports*, *59*(1), 1–37.

Cho, J., Rameshwar, P., & Sadoshima, J. (2009). Distinct roles of glycogen synthase kinase (GSK)-3alpha and GSK-3beta in mediating cardiomyocyte differentiation in murine bone marrow-derived mesenchymal stem cells. *The Journal of Biological Chemistry*, *284*(52), 36647–36658.

Doppler, S. A., Deutsch, M.-A., Lange, R., & Krane, M. (2013). Cardiac regeneration: Current therapies—Future concepts. *Journal of Thoracic Disease*, *5*(5), 683–697.

Forte, G., Pagliari, S., Ebara, M., Uto, K., Tam, J. K., Romanazzo, S., … Aoyagi, T. (2012). Substrate stiffness modulates gene expression and phenotype in neonatal cardiomyocytes in vitro. *Tissue Engineering Part A*, *18*(17-18), 1837–1848.

Gishto, A., Farrell, K., & Kothapalli, C. R. (2015). Tuning composition and architecture of biomimetic scaffolds for enhanced matrix synthesis by murine cardiomyocytes. *Journal of Biomedical Materials Research Part A*, *103*(2), 693–708.

Gnecchi, M., Danieli, P., & Cervio, E. (2012). Mesenchymal stem cell therapy for heart disease. *Vascular Pharmacology*, *57*(1), 48–55.

Goffin, J., & Eisenhauer, E. (2002). DNA methyltransferase inhibitors-state of the art. *Annals of Oncology*, *13*(11), 1699–1716.

Hafez, P., Jose, S., Chowdhury, S. R., Ng, M. H., Ruszymah, B. H., & Mohd, A. R. R. (2016). Cardiomyogenic differentiation of human sternal bone marrow mesenchymal stem cells using a combination of basic fibroblast growth factor and hydrocortisone. *Cell Biology International*, *40*(1), 55–64.

Hazeltine, L. B., Simmons, C. S., Salick, M. R., Lian, X., Badur, M. G., Han, W., … Pruitt, B. L. (2012). Effects of substrate mechanics on contractility of cardiomyocytes generated from human pluripotent stem cells. *International Journal of Cell Biology*, *2012*, 508294.

Hosoda, T. (2012). C-kit-positive cardiac stem cells and myocardial regeneration. *American Journal of Cardiovascular Disease*, *2*(1), 58–67.

Hou Lü, J. A. L., Liu, B. W., Xing, Y. J., Da, J., Hou, Z. L., & Ai, S. Y. (2013). Combination of BMP-2 and 5-AZA is advantageous in rat bone marrow-derived mesenchymal stem cells differentiation into cardiomyocytes. *Cell Biology International*, *37*(12), 1291–1299.

Jadczyk, T., Faulkner, A., & Madeddu, P. (2013). Stem cell therapy for cardiovascular disease: The demise of alchemy and rise of pharmacology. *British Journal of Pharmacology*, *169*(2), 247–268.

Joshi, J., & Kothapalli, C. R. (2015). Nanofibers based tissue engineering and drug delivery approaches for myocardial regeneration. *Current Pharmaceutical Design*, *21*(15), 2006–2020.

Karam, J.-P., Muscari, C., & Montero-Menei, C. N. (2012). Combining adult stem cells and polymeric devices for tissue engineering in infarcted myocardium. *Biomaterials*, *33*(23), 5683–5695.

Karantalis, V., Balkan, W., Schulman, I. H., Hatzistergos, K. E., & Hare, J. M. (2012). Cell-based therapy for prevention and reversal of myocardial remodeling. *American Journal of Physiology-Heart and Circulatory Physiology*, *303*(3), H256–H270.

Koyanagi, M., Bushoven, P., Iwasaki, M., Urbich, C., Zeiher, A. M., & Dimmeler, S. (2007). Notch signaling contributes to the expression of cardiac markers in human circulating progenitor cells. *Circulation Research*, *101*(11), 1139–1145.

Lakshmanan, R., Krishnan, U. M., & Sethuraman, S. (2012). Living cardiac patch: The elixir for cardiac regeneration. *Expert Opinion on Biological Therapy*, *12*(12), 1623–1640.

Lee, B., Zhou, X., Riching, K., Eliceiri, K. W., Keely, P. J., Guelcher, S. A., . . . Jiang, Y. (2014). A three-dimensional computational model of collagen network mechanics. *PLoS ONE*, *9*(11), e111896.

Li, Z., & Guan, J. (2011). Hydrogels for cardiac tissue engineering. *Polymers*, *3*(2), 740–761.

Lopez-Garcia, M. D., Beebe, D. J., & Crone, W. C. (2010). Young's modulus of collagen at slow displacement rates. *Bio-Medical Materials and Engineering*, *20*(6), 361–369.

Makino, S., Fukuda, K., Miyoshi, S., Konishi, F., Kodama, H., Pan, J., . . . Ogawa, S. (1999). Cardiomyocytes can be generated from marrow stromal cells in vitro. *The Journal of Clinical Investigation*, *103*(5), 697–705.

Martin-Rendon, E., Sweeney, D., Lu, F., Girdlestone, J., Navarrete, C., & Watt, S. M. (2008). 5-Azacytidine-treated human mesenchymal stem/progenitor cells derived from umbilical cord, cord blood and bone marrow do not generate cardiomyocytes in vitro at high frequencies. *Vox Sanguinis*, *95*(2), 137–148.

McMullen, N. M., & Pasumarthi, K. B. S. (2007). Donor cell transplantation for myocardial disease: Does it complement current pharmacological therapies? *Canadian Journal of Physiology and Pharmacology*, *85*(1), 1–15.

Parenteau-Bareil, R., Gauvin, R., & Berthod, F. (2010). Collagen-based biomaterials for tissue engineering applications. *Materials*, *3*(3), 1863–1887.

Pelouch, V., Dixon, I. M. C., Golfman, L., Beamish, R. E., & Dhalla, N. S. (1993). Role of extracellular matrix proteins in heart function. *Molecular and Cellular Biochemistry*, *129*(2), 101–120.

Perino, M. G., Yamanaka, S., Li, J., Wobus, A. M., & Boheler, K. R. (2008). Cardiomyogenic stem and progenitor cell plasticity and the dissection of cardiopoiesis. *Journal of Molecular and Cellular Cardiology*, *45*(4), 475–494.

Peterkin, T., Gibson, A., Loose, M., & Patient, R. (2005). The roles of GATA-4, -5 and -6 in vertebrate heart development. *Seminars in Cell and Developmental Biology*, *16*(1), 83–94.

Piryaei, A., Soleimani, M., Heidari, M. H., Saheli, M., Rohani, R., & Almasieh, M. (2015). Ultrastructural maturation of human bone marrow mesenchymal stem cells-derived cardiomyocytes under alternative induction of 5-azacytidine. *Cell Biology International*, *39*(5), 519–530.

Potapova, I. A., Doronin, S. V., Kelly, D. J., Rosen, A. B., Schuldt, A. J., Lu, Z., . . . Cohen, I. S. (2008). Enhanced recovery of mechanical function in the canine heart by seeding an extracellular matrix patch with mesenchymal stem cells committed to a cardiac lineage. *American Journal of Physiology-Heart and Circulatory Physiology*, *295*(6), H2257–H2263.

Qiu, Y., Bayomy, A. F., Gomez, M. V., Bauer, M., Du, P., Yang, Y., . . . Liao, R. (2015). A role for matrix stiffness in the regulation of cardiac side population cell function. *American Journal of Physiology-Heart and Circulatory Physiology*, *308*(9), H990–H997.

Ruan, Z. B., Zhu, L., Yin, Y. G., & Chen, G. C. (2010). The mechanism underlying the differentiation of human umbilical cord-derived mesenchymal stem cells into myocardial cells induced by 5-azacytidine. *Indian Journal of Medical Sciences*, *64*(9), 402–407.

Russo, V., Young, S., Hamilton, A., Amsden, B. G., & Flynn, L. E. (2014). Mesenchymal stem cell delivery strategies to promote cardiac regeneration following ischemic injury. *Biomaterials*, *35*(13), 3956–3974.

Sart, S., Tsai, A.-C., Li, Y., & Ma, T. (2014). Three-dimensional aggregates of mesenchymal stem cells: Cellular mechanisms, biological properties, and applications. *Tissue Engineering Part B, Reviews*, *20*(5), 365–380.

Sehnert, A. J., Huq, A., Weinstein, B. M., Walker, C., Fishman, M., & Stainier, D. Y. (2002). Cardiac troponin T is essential in sarcomere assembly and cardiac contractility. *Nature Genetics*, *31*(1), 106–110.

Seo, H. H., Lee, C. Y., Lee, J., Lim, S., Choi, E., Park, J. C., . . . Hwang, K. C. (2016). The role of nuclear factor of activated T cells during phorbol myristate acetate-induced cardiac differentiation of mesenchymal stem cells. *Stem Cell Research & Therapy*, *7*(1), 90.

Simmers, P., Gishto, A., Vyavahare, N., & Kothapalli, C. R. (2015). Nitric oxide stimulates matrix synthesis and deposition by adult human aortic smooth muscle cells within three-dimensional cocultures. *Tissue Engineering Part A*, *21*(7-8), 1455–1470.

Thiene, G., & Basso, C. (2010). Myocardial infarction: A paradigm of success in modern medicine. *Cardiovascular Pathology*, *19*(1), 1–5.

Valiente-Alandi, I., Schafer, A. E., & Blaxall, B. C. (2016). Extracellular matrix-mediated cellular communication in the heart. *Journal of Molecular and Cellular Cardiology*, *91*, 228–237.

Wang, F., & Guan, J. (2010). Cellular cardiomyoplasty and cardiac tissue engineering for myocardial therapy. *Advanced Drug Delivery Reviews*, *62*(7), 784–797.

Yang, Y.-, Leone, L. M., & Kaufman, L. J. (2009). Elastic moduli of collagen gels can be predicted from two-dimensional confocal microscopy. *Biophysical Journal*, *97*(7), 2051–2060.

Young, J. L., Kretchmer, K., Ondeck, M. G., Zambon, A. C., & Engler, A. J. (2014). Mechanosensitive kinases regulate stiffness-induced cardiomyocyte maturation. *Scientific Reports*, *4*, 6425.

Zimmermann, W. H., Didie, M., Doker, S., Melnychenko, I., Naito, H., Rogge, C., . . . Eschenhagen, T. (2006). Heart muscle engineering: An update on cardiac muscle replacement therapy. *Cardiovascular Research*, *71*(3), 419–429.

SUPPORTING INFORMATION

Additional supporting information may be found online in the Supporting Information section at the end of the article.

How to cite this article: Joshi J, Mahajan G, Kothapalli CR. Three-dimensional collagenous niche and azacytidine selectively promote time-dependent cardiomyogenesis from human bone marrow-derived MSC spheroids. *Biotechnology and Bioengineering*. 2018;1–14.
https://doi.org/10.1002/bit.26714